Eur. Phys. J. D (2012) 66: 97
DOI: 10.1140/epjd/e2012-20682-7

THE EUROPEAN PHYSICAL JOURNAL D

Regular Article

Quantum phase transition and dynamics induced by atom-pair tunnelling of Bose-Einstein condensates in a double-well potential

H. Cao[1] and L.B. Fu[2,3,a]

[1] School of Physics, Beijing Institute of Technology, Beijing 100081, P.R. China
[2] National Laboratory of Science and Technology on Computational Physics, Institute of Applied Physics and Computational Mathematics, Beijing 100088, P.R. China
[3] HEDPS, Center for Applied Physics and Technology, Peking University, Beijing 100084, P.R. China

Received 28 November 2011 / Received in final form 23 February 2012
Published online 19 April 2012 –

Abstract. We investigate the quantum phase transition (QPT) and dynamics induced by atom-pair tunnelling of Bose-Einstein condensates in a symmetric double well under the mean-field approximation. We find the system undergoes a new QPT towards phase-locking state when atom-pair tunnelling is strong enough, and the critical point of self-trapping QPT is shifted by atom-pair tunnelling. As for the dynamics, the system displays localized dynamical behaviour: phase-locking motion and self-trapping motion. We further study the correlation between this localized dynamics and QPT, and find that the area of the localized trajectories in the phase space can serve as an order parameter for both QPTs. The critical exponent of this order parameter is also discussed.

1 Introduction

As a widely tunable and well-controlled system [1,2] to model quantum tunnelling properties [3], Bose-Einstein condensates (BECs) in a symmetric double-well potential have attracted much attention both theoretically and experimentally. The BEC atoms may show highly asymmetric distribution as if most atoms are trapped in one well, even under a repulsive interaction between the degenerate atoms. This phenomenon, known as macroscopic quantum self-trapping [4–8], reveals the novel dynamical properties of the system.

Recently, direct observation of correlated tunnelling shows [9,10] that in the strong interaction regime, two atoms initially lying in either side of a double well will tunnel back and forth as a fragmented pair. Since the atom-pair tunnelling requires interaction of atoms in neighbouring wells that is not included in the two-site Bose-Hubbard model (TBHM), one should extend the TBHM to incorporate an atom-pair tunnelling term [11] in the Hamiltonian to describe this effect.

In this paper, we adopt a Hamiltonian including the atom-pair tunnelling term to describe BECs in a double-well potential [11]. In the mean-field approximation, we obtain the eigenstates and find two quantum phase transitions (QPTs) to self-trapping and phase-locking states, respectively. Furthermore, we study the dynamical transition from Josephson oscillation to two localized modes of motion (phase-locking motion and self-trapping motion), and establish the link between the dynamical transition and QPT. We find out that the area of both localized modes of motion in the phase space can be chosen as an order parameter. The scaling laws corresponding to these two QPTs are also discussed with this order parameter.

The rest of this paper is organized as follows. In Section 2 we present the model and an analysis of QPT in the mean-field approximation. Then we give a discussion of dynamical behaviour induced by atom-pair tunnelling in Section 3. Finally, our summary and conclusions are given in the last section.

2 Quantum phase transition

Taken the atom-atom interaction between neighbouring wells into account, the many-body second-quantized Hamiltonian for two weakly coupled BECs trapped in a symmetric double-well potential is given by [11]

$$H = \frac{c}{2N}(\hat{a}^\dagger\hat{a}^\dagger\hat{a}\hat{a} + \hat{b}^\dagger\hat{b}^\dagger\hat{b}\hat{b}) - \frac{v}{2}(\hat{a}^\dagger\hat{b} + \hat{b}^\dagger\hat{a}) + \frac{2\gamma c}{N}\hat{a}^\dagger\hat{a}\hat{b}^\dagger\hat{b} + \frac{\gamma c}{2N}(\hat{a}^\dagger\hat{a}^\dagger\hat{b}\hat{b} + \hat{b}^\dagger\hat{b}^\dagger\hat{a}\hat{a}) \quad (1)$$

where N is the total number of atoms, v is the effective Josephson coupling constant and c is the on-site

[a] e-mail: lbfu@iapcm.ac.cn

interaction strength. $\hat{a}^\dagger(\hat{b}^\dagger)$ and $\hat{a}(\hat{b})$ are the creation and annihilation operators for a bosonic particle in the ground state of either well. The change $v \to -v$ corresponds to the unitary transformation $\hat{a} \to \hat{a}$, $\hat{b} \to -\hat{b}$. Therefore, in this paper we mainly restrict our analysis to the case of $v \geq 0$. The last two terms result from the atom interaction between neighbouring wells, which is not included in TBHM, and the last term describes the atom-pair tunnelling. Here, we employ a factor $\gamma = \int dx\phi_a^2(x)\phi_b^2(x)/\int dx\phi_a^4(x)$ to describe the atom-pair correlation, where $\phi_{a,b}$ denotes the localized wavefunctions in either well. γ can be varied by adjusting the configuration of the double well, and is supposed to be small, around several percents for the present experimental technique. For the set-up in the experiment [9], γ is estimated to be 0.02 [11]. For simplicity, we set $\gamma = 0.02$ in most discussion of this paper.

For this second-quantized model, if the particle number is large enough, the system can be well described in the mean-field approximation [12,13]. In Hamiltonian (1), H/N is a constant in the limit of large particle number, and thus the parity effect [14] is not obvious. In this approximation, operators $\hat{a}$ and $\hat{b}$ can be replaced by two c-numbers $a = |a|e^{\mathrm{i}\theta_\mathrm{a}}$ and $b = |b|e^{\mathrm{i}\theta_\mathrm{b}}$. The quantity $|a|^2 + |b|^2$ is conserved and set to be unity. By introducing population imbalance $s = |b|^2 - |a|^2$ and relative phase $\theta = \theta_\mathrm{b} - \theta_\mathrm{a}$, the system can be described by a classical Hamiltonian [4,5]

$$H = \frac{\lambda(1-2\gamma)s^2}{4} - \frac{1}{2}\sqrt{1-s^2}\cos\theta + \frac{\gamma\lambda}{4}(1-s^2)\cos 2\theta, \tag{2}$$

with a constant term ignored, and $\lambda = c/v$. Here we have rescaled the energy with $v(>0)$. s and θ are a pair of canonically conjugate variables satisfying

$$\begin{cases} \dot{s} = -\frac{\partial H}{\partial \theta} = \frac{\gamma\lambda}{2}(1-s^2)\sin 2\theta - \frac{1}{2}\sqrt{1-s^2}\sin\theta, \\ \dot{\theta} = \frac{\partial H}{\partial s} = \frac{\lambda(1-2\gamma)s}{2} - \frac{\gamma\lambda s}{2}\cos 2\theta + \frac{s}{2\sqrt{1-s^2}}\cos\theta. \end{cases} \tag{3}$$

We at first review the case $\gamma = 0$. The fixed points, corresponding to the eigenstates of the system, can be readily derived from $\dot{s} = \dot{\theta} = 0$, and their solutions (s^*, θ^*) are relevant to the atom-interaction being repulsive or attractive. If atom-interaction is repulsive ($\lambda > 0$), the stable elliptic fixed point $(s^*, \theta^*) = (0, 0)$ is the ground state with energy $-1/2$, and the other elliptic fixed point $(0, \pi)$ is split into three: a hyperbolic fixed point $(0, \pi)$ (unstable) and two elliptic fixed points $(\pm\sqrt{1-\frac{1}{\lambda^2}}, \pi)$ when λ exceeds the critical value $\lambda_0 = 1$. Here, we denote self-trapping states as those eigenstates whose corresponding fixed points have a nonzero population imbalance, i.e. $s^* \neq 0$. Thus, these two fixed points $(\pm\sqrt{1-\frac{1}{\lambda^2}}, \pi)$ correspond to π-phase self-trapping states. For attractive atom-interaction ($\lambda < 0$), the system at the most attains four fixed points: $(0, 0)$ (elliptic), $(0, \pi)$ (elliptic when $|\lambda| < 1$, and hyperbolic when $|\lambda| > 1$), and $(\pm\sqrt{1-\frac{1}{\lambda^2}}, 0)$ (elliptic), among which the state $(0, 0)$ is the ground states for $|\lambda| < 1$, while the zero-phase self-trapping states $(\pm\sqrt{1-\frac{1}{\lambda^2}}, 0)$ represent doubly degenerate ground states for other cases. Therefore there is a QPT from non-degenerate to degenerate states at critical atom-interaction strength $\lambda = \lambda_0 = -1$ [7].

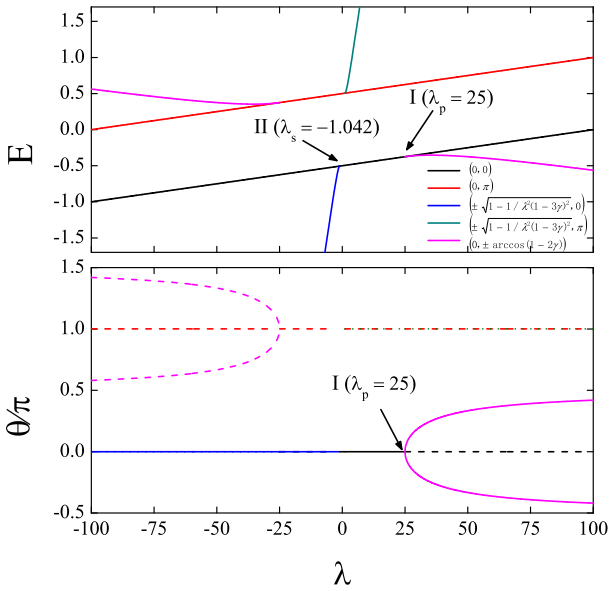

Fig. 1. (Color online) The eigen-energies E (upper panel) and the relative phase θ as an order parameter (lower panel, with lines in the corresponding colours) against λ with $\gamma = 0.02$. The solid lines in the lower panel represent the ground states of the system which undergoes a QPT between degenerate and non-degenerate state. The arrow I shows where the QPT to phase-locking state occurs, and the arrow II points out the self-trapping QPT point.

When $\gamma \neq 0$, there exist different eigenstates and thus different QPT points. We show the eigen-energies E and an order parameter θ in Figure 1. The system always attains fixed points $(0, 0)$ and $(0, \pi)$, both with increasing energies with respect to λ. When atom-interaction is repulsive ($\lambda > 0$), the state $(0, 0)$ is the ground state with energy $\frac{\gamma\lambda}{4} - \frac{1}{2}$ for $\lambda < \frac{1}{1-3\gamma}$. While $\lambda > \frac{1}{1-3\gamma}$, two degenerate π-phase self-trapping states $(\pm\sqrt{1-\frac{1}{\lambda^2(1-3\gamma)^2}}, \pi)$ emerge as the highest excited states. Compared with $\gamma = 0$, these two fixed points are shifted by atom-pair tunnelling. If atom-interaction is even stronger ($\lambda > \frac{1}{2\gamma}$), there appear another two elliptic fixed points $(0, \pm\arccos\frac{1}{2\lambda\gamma})$, which do not exist in the case $\gamma = 0$. These two states are the ground states, called phase-locking states with zero population imbalance and tunable relative phase unequal to 0 or π. Therefore, when $\lambda = \lambda_\mathrm{p} = \frac{1}{2\gamma}$ (marked with I in Fig. 1), the system undergoes a QPT from non-degenerate to degenerate states with symmetry breaking in relative phase. This QPT to phase-locking state was also investigated in [11].

If atom-interaction is attractive ($\lambda < 0$), there still exists the self-trapping QPT for $\gamma \neq 0$. When $|\lambda| < \frac{1}{1-3\gamma}$, the system only attains two eigenstates $(0, 0)$ and $(0, \pi)$, and the state $(0, 0)$ is the ground state. When $|\lambda|$ increases to a value greater than $\frac{1}{1-3\gamma}$, the

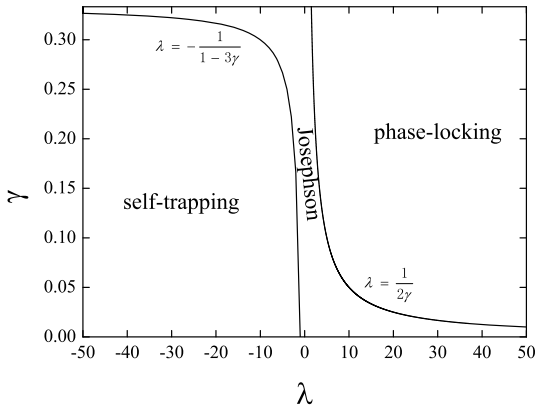

Fig. 2. Phase diagram as a function of λ and γ. The phase boundaries are determined by curves $\lambda = -\frac{1}{1-3\ \gamma}$ and $\lambda = \frac{1}{2\gamma}$.

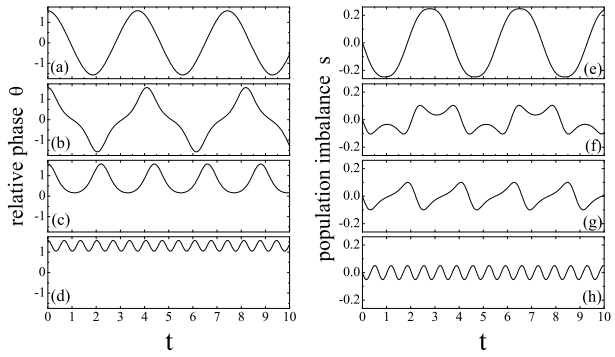

Fig. 3. Relative phase θ (left column) and population imbalance s (right column) as a function of time t with initial conditions $\theta(0) = \pi/2$ and $s(0) = 0$. $\gamma = 0.02$. From top to bottom, λ takes on 20 (a, e), 49 (b, f), 51 (c, g) and 100 (d, h), respectively.

emerging states $(\pm\sqrt{1 - \frac{1}{\lambda^2(1-3\gamma)^2}}, 0)$ become the doubly-degenerate ground states with energies decreasing rapidly with increasing $|\lambda|$, and correspond to zero-phase self-trapping states. As $|\lambda|$ increases further to exceed $\frac{1}{2\gamma}$, there appear two more eigenstates $(0, \pm\arccos\frac{1}{2\lambda\gamma})$ (elliptic fixed points). However, these two states represent the highest excited states, and thus the ground states remain unchanged. Therefore, when $\lambda = \lambda_s = -\frac{1}{1-3\gamma}$, the system undergoes a QPT to a symmetry breaking phase in population imbalance. In Figure 1, we can also see the change of energy level structures corresponding to the QPT to self-trapping state at small $|\lambda|$ region.

The knowledge of eigenstates above enables us to depict the phase diagram shown in Figure 2. The parameter space (λ, γ) is divided into three regions: self-trapping, Josephson, and phase-locking. As γ is usually small in the experiments of BECs in a double well, phase-locking states exist only when the atom-interaction is very strong. For example, in the experiment in [9], γ is approximate to 0.02 [11], and thus one should tune the atom-interaction strength λ to exceed 25 to observe the phase-locking states. The relative phase in the phase-locking state increases or decreases monotonically on the atom-interaction strength, which suggests a potential way of phase control.

3 Dynamics

It is well known that in TBHM, when atom-interaction is strong, the system will display self-trapping motion. Different from the Josephson oscillation with zero time-average of both population imbalance and relative phase, the time-average of population imbalance becomes nonzero in the self-trapping motion. Specifically, for an initial condition with $s(0) = 1$ indicating that all the BEC atoms are initially lying in one side of a double well, the population imbalance in self-trapping motion is localized to oscillate between 0 and 1, leading to a nonzero time-average of population imbalance, i.e. $\langle s \rangle \neq 0$. When atom-pair tunnelling is taken into consideration, strong atom-interaction would induce new modes of motion similar to self-trapping motion but localized in relative phase θ. These modes of motion are called phase-locking motion shown as an oscillation with the time-average of relative phase unequal to 0 or π and a zero time-average of population imbalance.

In Figure 3 we show the evolution of the relative phase θ and the population imbalance s for certain initial conditions $\theta(0) = \pi/2$ and $s(0) = 0$ in different atom-interaction strength $\lambda = 20$, 49, 51 and 100, respectively. Here we suppose $\gamma = 0.02$. As can be seen from the figure, for these initial conditions, the critical value for this dynamical transition is $\lambda_c = 50$. When λ is far below the critical value (Figs. 3a, 3e), the relative phase oscillates between $\pi/2$ and $-\pi/2$ in a sine-like way. As λ approaches the critical value, multi-frequency oscillations become evident for both s and θ (Figs. 3b, 3f). When λ exceeds the critical value (Figs. 3c–3d, 3g–3h), the motion of relative phase is restricted in the $(0, \pi)$ range and the population imbalance oscillates around zero with a small amplitude. That is, there emerge the phase-locking modes. The oscillation amplitude of the relative phase decreases with increasing atom-interaction strength, which results into an increasing time-average of the relative phase.

This dynamical transition can be well understood with the help of the phase space of the classical Hamiltonian (2). In Figure 4a we plot the phase-space trajectories and classical energy profiles with $\gamma = 0.02$ in different atom-interaction strength $\lambda = 20$, 50, and 100. The black dots denote the fixed points. The energy profiles suggest that the relative phase θ can be regarded as a spatial coordinate of a quasi-particle in a potential. Note that the local extremes of this potential correspond to the fixed points. That is, when this potential changes from a single well into a symmetric double well, it gives rise to a symmetry breaking of the system, and the corresponding fixed point occurs a bifurcation, which signifies the QPT at $\lambda = \lambda_p$. This critical value $\lambda = \lambda_p$ is always less than the dynamical transition point λ_c (to be evaluated below) in absolute magnitude, since the latter depends on the initial energy of the quasi-particle as well as the

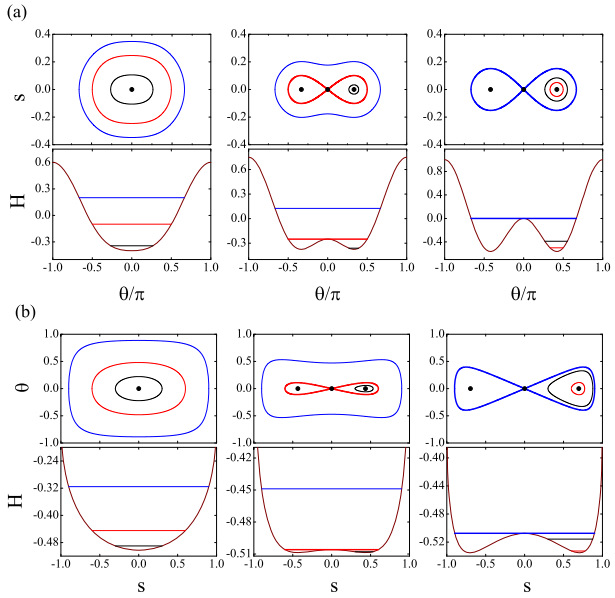

Fig. 4. (Color online) The phase-space trajectories (upper panels) and the energy profiles (lower panels, with the lines in the corresponding colours) of classical Hamiltonian (2) for $\gamma = 0.02$. The black dots denote the fixed points. (a) The atom-interaction strength $\lambda = 20$, 50, 100 from left to right. The red lines are the trajectories with initial conditions $s(0) = 0$ and $\theta(0) = \frac{\pi}{2}$. (b) The atom-interaction strength $\lambda = -0.5, -1.182, -1.482$ from left to right. The red lines are the trajectories with initial conditions $s(0) = 0.6$ and $\theta(0) = 0$.

configurational change of the potential. It is clear that the dynamical transition occurs at the moment when the energy $H(0, \frac{\pi}{2}) = -\frac{\lambda\gamma}{4}$ of the trajectory with these initial conditions $s(0) = 0$ and $\theta(0) = \frac{\pi}{2}$ equals the separatrix $H = H(0,0) = -\frac{1}{2} + \frac{\lambda\gamma}{4}$. If the energy of the trajectory with certain initial conditions is less than the potential barrier height $H(0,0)$, the relative phase is localized to oscillate only in one side of $\theta = 0$, i.e., phase-locking motion happens. Thus, when $\lambda > 0$, for given initial conditions $s(0)$ and $\theta(0)$, the phase-locking motion occurs when

$$H_0 = H(s(0), \theta(0)) < H(0,0), \tag{4}$$

and the critical parameter is

$$\lambda_c = \frac{2(\sqrt{1-s^2(0)}\cos\theta(0) - 1)}{(1-2\gamma)s^2(0) + \gamma(1-s^2(0))\cos 2\theta(0) - \gamma}. \tag{5}$$

For comparison, we also plot in Figure 4b the phase trajectories and energy profiles for attractive atom-interaction ($\lambda < 0$). The atom-interaction strength takes on -0.5, -1.182, and -1.482, respectively, and $\gamma = 0.02$. Following a similar analysis, we can draw the conclusion that the same condition in (4) along with the limitation $\lambda < 0$ leads to the self-trapping motion [7,15].

On the other hand, with λ and γ remaining constant, equation (4) determines the critical trajectories with energy $H_c = H(0,0)$, shown as thick lines in Figure 4, inside which the system undergoes phase-locking motion or self-trapping motion. Let us denote A as the area enclosed by

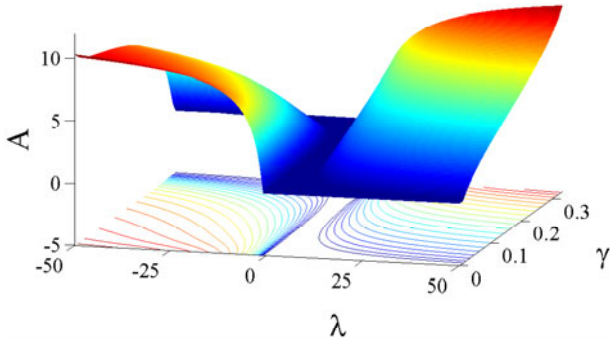

Fig. 5. (Color online) The area A of localized modes and its contour projection on the (λ, γ) parameter space.

the critical trajectory, namely for phase-locking motion,

$$A = 2\int_{-\theta_c}^{\theta_c} s(\theta)d\theta, \tag{6}$$

with

$$s(\theta) = \left[1 - \left(-\frac{\cos\theta}{\lambda(1-2\gamma-\gamma\cos 2\theta)} + \sqrt{\frac{\lambda(1-3\gamma)+2}{\lambda(1-2\gamma-\gamma\cos 2\theta)} + \frac{\cos^2\theta}{\lambda^2(1-2\gamma-\gamma\cos 2\theta)^2}}\right)^2\right]^{1/2},$$

and $\theta_c = \arccos(\frac{1}{\lambda\gamma} - 1)$ is the critical relative phase when $s = 0$.

For self-trapping motion,

$$A = 2\int_{-s_c}^{s_c} \theta(s)ds, \tag{7}$$

with

$$\theta(s) = \arccos\frac{1 - \sqrt{-2\gamma\lambda^2(1-\gamma)s^2 + (2\gamma\lambda - 1)^2}}{2\gamma\lambda\sqrt{1-s^2}}, \tag{8}$$

and $s_c = \sqrt{1 - (1 + \frac{2}{\lambda(1-3\gamma)})^2}$ is the critical population imbalance when $\theta = 0$. Note that the variable A in equations (6) and (7) is indeed the classical action of the trajectory.

For Josephson region, i.e., there is no localized modes, then $A = 0$ since $s_c = 0$. Indeed, the variable A represents the area of localized modes in the phase-space. In Figure 5 we plot A and its contour projection as a function of λ and γ. The (λ, γ) space is divided into three regions: two nonzero-valued regions separated by a zero-valued region, and the separatrices are the same as the phase boundaries in Figure 2.

In this way, these three dynamical regions are consistent with those regions in the phase diagram. We can seek for an understanding from the trajectories in the phase space in Figure 4. When $\lambda < \lambda_p$, there only exist closed

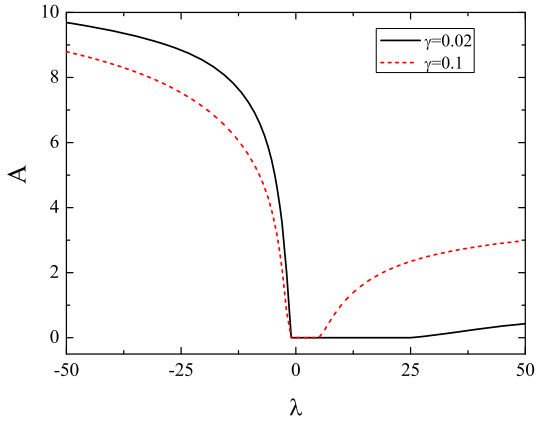

Fig. 6. The area A of localized modes as a function of λ shown as a good order parameter. The area A undergoes two transitions from zero to nonzero values symbolizing two QPTs. To show this behavior clearer, we plot the line for $\gamma = 0.1$ besides the previously used $\gamma = 0.02$.

trajectories around fixed points $(0, 0)$. The area of localized modes is zero, i.e., $A = 0$. Then on crossing $\lambda_{\rm p}$, the fixed point bifurcation is accompanied by the central point change of a portion of trajectories, and thus the area A of localized modes changes from zero to nonzero value. To show this property clear, we plot A as a function of λ for the cases $\gamma = 0.02$ and 0.1 in Figure 6 for example. This variable undergoes two transitions from zero to nonzero values at $\lambda = \frac{1}{2\gamma}$ and $-\frac{1}{1-3\gamma}$ corresponding to the two QPTs, which suggests the quantity A can be chosen as an order parameter.

For a quantity playing the role of an order parameter, its scaling behaviour in the vicinity of the critical point is of interest, which is characterized by critical exponents [16]. For instance, if we expand the previously mentioned order parameter θ in the vicinity of critical point $\lambda_{\rm p}$, then we will find that it scales like $\theta \propto |\lambda - \lambda_{\rm p}|^{\beta}$, where the critical exponent $\beta = 1/2$ for $\lambda \to \lambda_{\rm p}^{+}$, and $\beta = 0$ for $\lambda \to \lambda_{\rm p}^{-}$. Similarly, it can be easily obtained that the order parameter s for the self-trapping QPT scales like $s \propto |\lambda - \lambda_{\rm s}|^{\beta}$, where $\beta = 1/2$ for $\lambda \to \lambda_{\rm s}^{-}$ and $\beta = 0$ for $\lambda \to \lambda_{\rm s}^{+}$. This same critical exponent again suggests the connection of the two QPTs. As for the proposed order parameter A, we assume it also has similar scaling behaviour, i.e. $A \propto |\lambda - \lambda_{\rm p,s}|^{\alpha}$ in both the vicinities of $\lambda_{\rm p}$ and $\lambda_{\rm s}$. To evaluate the critical exponent α, we numerically calculate the integral in (6) in the vicinity of the critical point $\lambda_{\rm p}$ and that in (7) in the vicinity of the critical point $\lambda_{\rm s}$. In Figure 7 we show the area A as a function of $(\lambda - \lambda_{\rm p,s})/\lambda_{\rm p,s}$ for various γ in the logarithmic scale, and they are shown as straight lines with the same slope 3/2 for both $\lambda \to \lambda_{\rm p}^{+}$ and $\lambda \to \lambda_{\rm s}^{-}$ for different values of γ. It suggests that in the vicinity of critical points the area A indeed scales like $A \propto |\lambda - \lambda_{\rm p,s}|^{\alpha}$, where the critical exponent $\alpha = 3/2$ is independent of γ in both the phase-locking and self-trapping regime. This order parameter can then be regarded as universal, and phase-locking and self-trapping phase transition may be classified into the same class of phase transition.

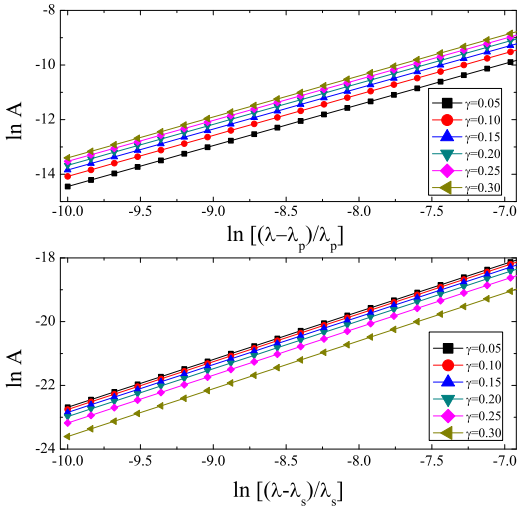

Fig. 7. (Color online) The area A of localized modes versus λ with various γ. For both phase-locking motion (upper panel) and self-trapping motion (lower panel), the critical component $\alpha = 3/2$ for different values of γ.

4 Conclusion

In conclusion, by the model Hamiltonian including the atom-pair tunnelling term, we investigate the effect of atom-pair tunnelling on the phase transition and dynamics of BECs in a symmetric double-well potential in the mean-field approximation. We find that atom-pair tunnelling results in a phase transition towards the phase-locking state, and shifts the phase transition point of self-trapping. The system also exhibits new localized mode of motion, i.e. phase-locking motion, which along with the Josephson motion and self-trapping motion divides the parameter space into three dynamical regions. We make a connection between these regions and different phases in the phase diagram. In two of these three dynamical regions, the system displays localized modes of motion. We find that the area of localized modes is indeed the classical action and turns out to be a candidate for the order parameter. Since the action is related to the Landau-Zener tunneling rate [17], the newly proposed order parameter is likely to be experimentally measurable. With this parameter, we discuss the scaling behavior of the two phase transitions, and find out that they have the same critical exponent, which suggests that these two phase transitions may be regarded in the same class.

This work is supported by the National Fundamental Research Program of China (Contact Nos. 2007CB814800 and 2011CB921503), the National Natural Science Foundation of China (Contact Nos. 10725521, 91021021, 11075020, and 11078001).

References

1. F. Dalfovo, S. Giorgini, L.P. Pitaevskii, S. Stringari, Rev. Mod. Phys. **71**, 463 (1999)
2. A.J. Leggett, Rev. Mod. Phys. **73**, 307 (2001)
3. M. Grifoni, P. Hänggi, Phys. Rep. **304**, 229 (1998)

4. G.J. Milbrun, J. Corney, E.M. Wright, D.F. Walls, Phys. Rev. A **55**, 4318 (1997)
5. A. Smerzi, S. Fantoni, S. Giovanazzi, S.R. Shenoy, Phys. Rev. Lett. **79**, 4950 (1997)
6. I. Marino, S. Raghavan, S. Fantoni, S.R. Shenoy, A. Smerzi, Phys. Rev. A **60**, 487 (1999)
7. S. Raghavan, A. Smerzi, S. Fantoni, S.R. Shenoy, Phys. Rev. A **59**, 620 (1999)
8. M. Albiez, R. Gati, S. Fölling, S. Hunsmann, M. Cristiani, M.K. Oberthaler, Phys. Rev. Lett. **95**, 010402 (2005)
9. S. Fölling, S. Trotzky, P. Cheinet, M. Feld, R. Saers, A. Widera, T. Müller, I. Bloch, Nature **448**, 1029 (2007)
10. S. Zöllner, H.-D. Meyer, P. Schmelcher, Phys. Rev. Lett. **100**, 040401 (2008)
11. J.-Q. Liang, J.-L. Liu, W.-D. Li, Z.-J. Li, Phys. Rev. A **79**, 033617 (2009)
12. D. Ananikian, T. Bergeman, Phys. Rev. A **73**, 013604 (2006)
13. B. Wu, J. Liu, Phys. Rev. Lett. **96**, 020405 (2006)
14. D.V. Averin, T. Bergeman, P.R. Hosur, C. Bruder, Phys. Rev. A **78**, 031601 (2008)
15. L.-B. Fu, J. Liu, Phys. Rev. A **74**, 063614 (2006)
16. M.A. Continentino, *Quantum Scaling in Many-Body Systems* (World Scientific Publishing Co. Pte. Ltd., Singapore, 2001), p. 4
17. J. Liu, L.-B. Fu, B.-Y. Ou, S.-G. Chen, B. Wu, Q. Niu, Phys. Rev. A **66**, 023404 (2002)